MOLECULAR AND CELLULAR BIOLOGY, Apr. 1996, p. 1509–1518 Vol. 16, No. 4
0270-7306/96/$04.00+0

Two Chimeric Receptors of Epidermal Growth Factor Receptor and c-Ros That Differ in Their Transmembrane Domains Have Opposite Effects on Cell Growth

QINGHUA XIONG, JOSEPH L.-K. CHAN, CONG S. ZONG, AND LU-HAI WANG*

Department of Microbiology, Mount Sinai School of Medicine, New York, New York 10029

Received 27 September 1995/Returned for modification 11 November 1995/Accepted 28 January 1996

Two chimeric receptors, ER1 and ER2, were constructed. ER1 contains the extracellular and transmembrane (TM) domains derived from epidermal growth factor receptor and the cytoplasmic domain from c-Ros; ER2 is identical to ER1 except that its TM domain is derived from c-Ros. Both chimeras can be activated by epidermal growth factor and are capable of activating or phosphorylating an array of cellular signaling proteins. Both chimeras promote colony formation in soft agar with about equal efficiency. Surprisingly, ER1 inhibits while ER2 stimulates cell growth on monolayer culture. Cell cycle analysis revealed that all phases, in particular the S and G_2/M phases, of the cell cycle in ER1 cells were elongated whereas G_1 phase of ER2 cells was shortened threefold. Comparison of signaling pathways mediated by the two chimeras revealed several differences. Several early signaling proteins are activated or phosphorylated to a higher extent in ER1 than in ER2 cells in response to epidermal growth factor. ER1 is less efficiently internalized and remains tyrosine phosphorylated for a longer time than ER2. However, phosphorylation of the 66-kDa Shc protein, activation of mitogen-activated protein kinase, and induction of c-*fos* and c-*jun* occur either to a lesser extent or for a shorter time in ER1 cells. Cellular protein phosphorylation patterns are also different in ER1 and ER2 cells. In particular, a 190-kDa Shc-associated protein is tyrosine phosphorylated in ER2 but not in ER1 cells. Our results indicate that the TM domains have a profound effect on the signal transduction and biological activity of those chimeric receptors. The results also imply that sustained stimulation of ER1 due to its retarded internalization apparently triggers an inhibitory response that dominantly counteracts the receptor-mediated mitogenic signals. These two chimeras, expressed at similar levels in the same cell type but having opposite effects on cell growth, provide an ideal system to study the mechanism by which a protein tyrosine kinase inhibits cell growth.

Receptor protein tyrosine kinase (RPTK) plays an important role in regulation of cell growth, differentiation, and metabolism. The binding of a ligand to an RPTK leads to activation of its kinase activity, resulting in self-phosphorylation and causing a series of cellular proteins involved in signal transduction to elicit diverse effects (4, 5). Although overwhelming evidence demonstrates that RPTKs are involved in promoting cell growth and transformation, they may also inhibit cell growth and induce differentiation in certain cell types. Epidermal growth factor receptor (EGFR) is known to stimulate cell growth of a number of cell types but inhibit growth of A431 cells upon stimulation (12, 13, 19, 29). Overexpression of insulin or EGF receptors in PC12 cells has been shown to induce their differentiation rather than proliferation (9, 50). Much progress has been made in understanding the mechanism by which an RPTK promotes cell growth, but the mechanism of growth inhibition and cell differentiation remains largely unknown.

Chicken c-*ros* codes for an RPTK of 2,311 amino acids (aa) sharing homology with *sevenless* of *Drosophila melanogaster* and insulin receptor (IR) family RPTKs (2, 5, 32). Temporally controlled and epithelially restricted expression of c-*ros* in several organs suggests that it may play some role in epithelium differentiation during embryogenesis as well as in the physiological function of these mature organs (6, 47, 49). Besides the spontaneous transduction and activation of its tumorigenic potential in avian sarcoma virus UR2, c-*ros* was implicated in the development of human glioblastomas as an elevated level of c-*ros* expression or rearranged c-*ros* products were found in most of the established glioblastoma cell lines (3). Further study of the biochemical and biological properties of c-*ros* has been hindered by the difficulty of its expression in mammalian cell lines (5b) and the lack of knowledge of its putative ligand.

Chimeric receptors have been successfully used to study the receptors or receptor-like proteins without known ligands. By using such an approach, several functional chimeras between different pairs of RPTKs have been created, including IR-Ros, EGFR-NGFR, EGFR-ErbB2, EGFR-Neu, EGFR-Kit, EGFR-Ret, EGFR-ELK, EGFR-IR, IR-EGFR, IR-IGFR, IGFR-IR, and NGFR-Ros (1, 8, 25–28, 36, 40–42, 52). Studies on the IR-EGFR and IR-IGFR chimeric receptors (26, 40) concluded that it is the cytoplasmic domain that determines the signaling specificity. The function of the transmembrane (TM) domains of RPTKs has also been assessed by using chimeric receptors. The chimeric EGFR-$p75^{NGFR}$ receptor with its TM and cytoplasmic domains derived from $p75^{NGFR}$ was shown to be able to induce differentiation of PC12 cells in response to EGF, whereas the other chimera with the TM domain from EGFR was unable to do so (52). Our earlier study showed that removal of a 3-aa insertion in the TM domain of v-Ros resulted in an altered pattern of its substrate interaction and transforming ability (54). Those observations suggest that the TM domain may play a significant role in signal transduction other than merely serving as a membrane anchor.

In this report, we have studied the function of c-Ros in cultured cells by using chimeric receptors of EGFR and c-Ros. Our results showed that the two chimeras, ER1 and ER2, which differ in their TM domains, have similar abilities in promoting colony formation of the expressing cells in soft agar

* Corresponding author. Phone: (212) 241-3795. Fax: (212) 534-1684.

but have opposite effects on cell growth on monolayer culture. Comparison of signaling pathways mediated by the two chimeras has revealed differences that may account for their opposite effects on cell growth.

MATERIALS AND METHODS

Cells and colony formation assay. NIH 3T3 cells were maintained in Dulbecco modified Eagle medium with 5% calf serum. The colony formation assay was performed according to the published method (18). If EGF was included in the assay, EGF containing soft agar medium (0.5% serum) was overlaid every 5 days and the control plate was overlaid with soft agar medium only.

Antibodies. Anti-Ros antibody (Ab) 219 (21) and anti-IRS1 Ab (20a) were made in our laboratory. Antiphosphotyrosine Ab 4G10 and anti-phospholipase Cγ (anti-PLCγ) anti-Shc, and anti-EGFR (clone LA 22) Abs were purchased from Upstate Biotechnology Inc. Anti-ERK-1 (C-16) was from Santa Cruz Biotechnology. Anti-mitogen-activated protein (MAP) kinase Ab TR-10 was a gift from Michael Weber. RC-20, a recombinant anti-p-Tyr immunoglobulin G conjugated with alkaline phosphatase was purchased from Transduction Laboratories. Goat anti-rabbit immunoglobulin G and rabbit anti-mouse immunoglobulin G conjugated with alkaline phosphatase were purchased from Boehringer Mannheim.

Construction of expression plasmids. Two chimeric receptors, ER1 and ER2, were constructed. To construct the ER1 expression plasmid (Fig. 1), the plasmid pZIPER containing the full-length coding sequence of human EGFR (a gift from M. Shibuya) was digested first with *Sac*I and then partially with *Nar*I to release the *Sac*I-*Nar*I fragment (aa −24 to 646). The cytoplasmic domain of c-*ros* was generated by PCR from the pECEROS plasmid (5a) by using the following pair of primers. Primer 1, 5′ *CGAAGGCGCCA*AAGATGGAAATCCAGA, contains the sequence of EGFR (italic) and the *Nar*I recognition site (underlined) at its 5′ end followed by the c-*ros* sequence corresponding to the region immediately carboxyl to its TM domain (5). Primer 2, 5′ CCGGATCCTCTAGACTCTCTT CTGTCCTCAAACAG, corresponds to the 3′ noncoding region of c-*ros* and contains an *Xba*I site (underlined). The PCR product was first digested with *Nar*I and *Xba*I and then ligated together with the *Sac*I-*Nar*I fragment of EGFR to the pBluescript vector at the *Sac*I and *Xba*I sites. The resulting plasmid containing the extracellular (EC) and TM domain of EGFR and cytoplasmic domain of c-Ros was confirmed by sequencing the whole PCR region. The chimeric cDNA was then released from pBluescript and ligated to a mammalian expression vector, pECE, that contains a simian virus 40 promoter (10). The ER2 that has the EC domain of c-Ros replaced by the corresponding region of EGFR was constructed as follows (Fig. 1). A *Sac*I-*Bst*XI fragment (aa −24 to 625) coding for the EC domain of EGFR was released from pZIPER. A junction fragment bridging the EC domain of EGFR and the c-*ros* sequence was generated by PCR with the following pair of primers: primer 3, 5′ *CATCGCCACTGGGATGG*AT ATCACTACTGCTATTGTTGCT, contains the sequence of EGFR (italic) including the *Bst*XI recognition site (underlined) and the c-Ros sequence corresponding to the TM domain; and primer 4, 5′ CTCTGCTTGAGAAGGAAGA GTGCT, corresponds to c-Ros (aa 1941 to 1949) in the cytoplasmic domain and includes the *Ear*I recognition site (underlined). The PCR fragment was digested with *Bst*XI and *Ear*I. An *Ear*I-*Not*I cDNA fragment corresponding to the 3′ cytoplasmic region of c-Ros, together with the PCR junction fragment and the EGFR *Sac*I-*Bst*XI fragment corresponding to its EC domain, was ligated to pBluescript (SK^+) vector at *Sac*I-*Not*I sites. The resulting plasmid containing the EGFR-*ros* fragment was confirmed by sequencing the PCR fragment and junction regions. The EGFR-*ros* fragment was then transferred to pECE vector at *Sac*I-*Xba*I sites.

Transfection and selection of cell lines. DNA transfection by calcium phosphate was done as described elsewhere (16, 53, 54).

Protein analysis. Protein extraction, subcellular fractionation, immunoprecipitation (IP), sodium dodecyl sulfate-polyacrylamide gel electrophoresis (SDS-PAGE), in vitro kinase assay, phosphatidylinositol (PI) 3-kinase assay, and detection of surface proteins were done according to published procedures (11, 21–23, 30, 53, 54).

EGF binding. Cells were plated in 6- or 10-cm dishes at 1×10^6 to 2×10^6 or 3×10^6 to 4×10^6 cells per dish, respectively. The following day, plates were placed on ice and washed with cold phosphate-buffered saline (PBS)–bovine serum albumin (BSA) (1 mg of BSA per ml). Cells were then incubated with 20 ng of ^{125}I-EGF per ml with varying concentrations and up to 50-fold excess of cold EGF in 1 ml of PBS-BSA for 2 h at 4°C. At the end of binding, cells were washed with PBS-BSA three times and then lysed in 0.5 ml of a solution containing 0.2% SDS and 0.2 N NaOH. The total lysates were collected and measured for radioactivity.

MAP kinase assay. Cell lysates were immunoprecipitated with the TR-10 Ab washed three times with radio immunoprecipitation assay buffer and once with the MAP kinase assay buffer (10 mM Tris-HCl [pH 7.5], 10 mM magnesium acetate), resuspended in 20 μl of the same assay buffer, and then mixed with 20 μl of myelin basic protein (2 mg/ml). The reaction was started by the addition of 20 μl of 3× hot mix (5 μCi of [γ-^{32}P]ATP per reaction mixture, 150 μM ATP, 30 mM magnesium acetate, 30 mM HEPES [*N*-2-hydroxyethylpiperazine-*N*′-2-ethanesulfonic acid] [pH 7.5]) and incubated at 30°C for 30 min. The reaction was stopped by addition of SDS-PAGE sample buffer, and the mixture was boiled for 5 min. The sample was centrifuged at 16,000 × *g* briefly, and the supernatant was loaded onto an SDS–15% polyacrylamide gel and then electrophoresed and autoradiographed.

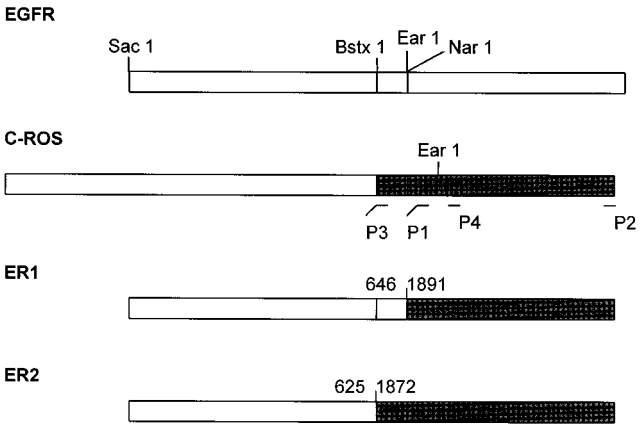

FIG. 1. Construction of ER1 and ER2 chimeras. Structures of EGFR, c-Ros, and chimeras ER1 and ER2 are shown. ER1 has the EC and TM domains of EGFR (aa −24 to 646) fused to the cytoplasmic domain of c-Ros (aa 1891 to 2311) whereas ER2 has the EC domain of c-Ros replaced by that of EGFR (aa −24 to 625).

Flow cytometry analysis. Cells were trypsinized, resuspended in PBS, and fixed with ethanol at a final concentration of 70% by adding ethanol dropwise while vortexing. Cells were then kept at 4°C. Before flow cytometry analysis, cells were pelleted by centrifugation at 600 × *g* for 10 min and digested with RNase A (2 mg/ml) in 250 μl of PBS for at least 30 min at 37°C and then stained with propidium iodide staining solution (10× stock solution containing 0.5 mg of propidium iodide per ml, 10 mg of sodium citrate per ml, and 1% Triton X-100) for 30 min at room temperature.

RNA slot blot analysis. Total RNA was extracted from cells by using RNAZOL B reagent according to the manufacturer's protocol (TEL-TEST, Inc.). RNA slot blot was prepared by using a Minifold II apparatus according to the manufacturer's instructions (Schleicher & Schuell). Prehybridization and hybridization were carried out in a solution containing 50% formamide, 6× SSC (1× SSC is 0.15 M NaCl plus 0.015 M sodium citrate), 5× Denhardt's solution, 0.5% SDS, and 100 μg of salmon sperm DNA per ml (and an appropriate amount of ^{32}P-labeled cDNA probes in the case of hybridization) at 42°C for 2 h and overnight, respectively. Filters were washed in 0.1× SSC–0.2% SDS at 62°C for 30 min. cDNA probes were labeled with a random priming kit (New England Biolabs). Human c-*jun* cDNA and rat c-*fos* cDNA were gifts from Irwin Gelman and Selina Chen-Kiang, respectively.

RESULTS

Construction and expression of chimeric EGFR-Ros receptors. Two EGFR-Ros chimeras which differ only in their TM domains were constructed (Fig. 1). One of them, named ER1, has the entire EC and TM domains of EGFR, including 2 aa residues carboxyl terminal to the TM domain (aa residues −24 to 646 of EGFR) fused to c-Ros at the cytoplasmic border of its TM domain (aa residues 1891 to 2311) (5). The other one, ER2, has the entire EC domain (aa residues −24 to 625) of EGFR joined at the EC border of the TM domain of c-Ros (aa residues 1872 to 2311). The chimeras are placed under the control of the simian virus 40 promoter in a mammalian expression vector, pECE. To establish stable expression cell lines, pER1 or pER2, together with a pSV2-Neo plasmid containing the geneticin resistance gene, was transfected into NIH 3T3 cells. After selection with geneticin, the resistant colonies were picked, amplified, and analyzed for ER1 and ER2 expression by Western blotting (immunoblotting) with anti-Ros Ab. A broad band with an apparent molecular mass of about 160 kDa was detected (data not shown).

The chimera protein expression levels of independent ER1 and ER2 clones were compared and found to have similar

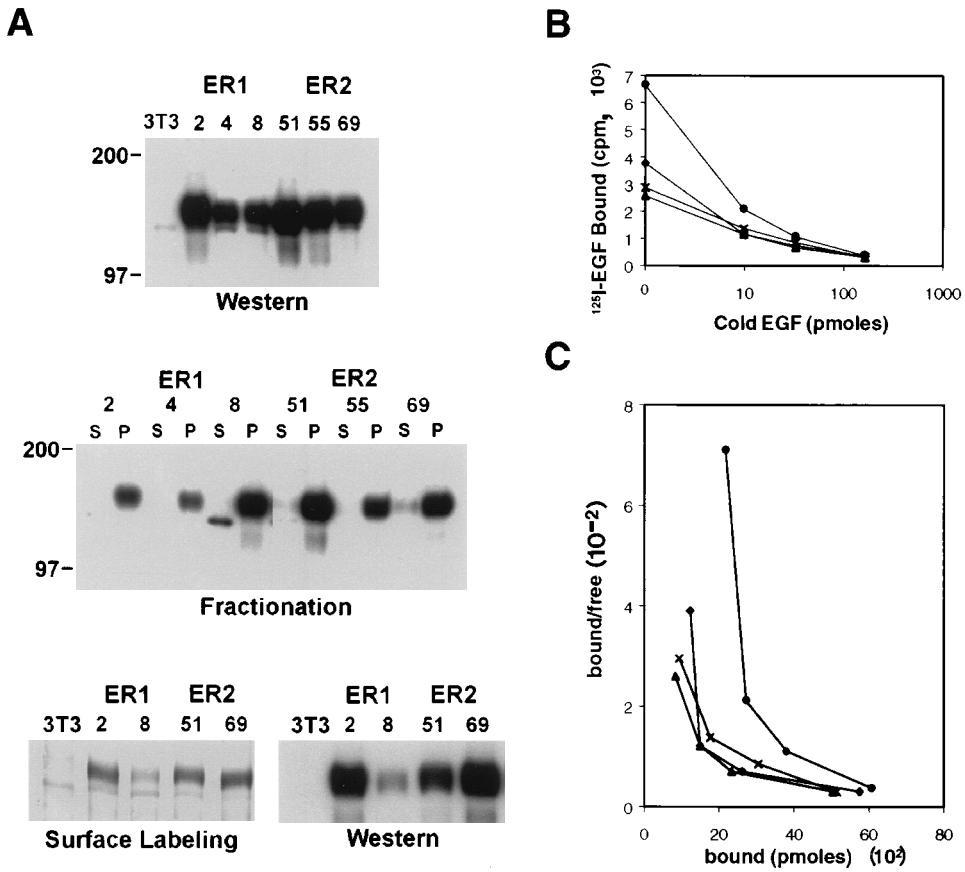

FIG. 2. Expression, subcellular localization, and EGF binding of ER1 and ER2 chimeras. (A) Expression levels and subcellular localization of ER1 and ER2 receptors. Top panel, equivalent amounts (500 μg) of total cell extracts from control 3T3 cells as well as cells of independent ER1 (no. 2, 4, and 8) and ER2 (no. 51, 55, and 69) clones were immunoprecipitated, separated by SDS-PAGE, and blotted with anti-Ros Ab. Middle panel, cell extracts from one confluent 10-cm dish each of ER1 and ER2 cells were fractionated into S100 and P100 fractions and analyzed similarly as the top panel. Numbers to the left of the top and middle panels indicate molecular mass in kilodaltons. Bottom panel, the intact cells were labeled with sulfo-*N*-hydroxysulfosuccinimide-LC-biotin and extracted as described before (53). The extracts were immunoprecipitated with anti-Ros Ab. Duplicate aliquots were analyzed by SDS-PAGE, blotted, and detected with alkaline phosphatase-coupled avidin (left panel) or anti-Ros Ab (right panel). (B) EGF binding of ER1 and ER2 chimeric receptors. Duplicate 6-cm dishes or 10-cm dishes of ER1 (clones 2 and 8) and ER2 (clones 57 and 69) cells were used for EGF binding analysis as described in Materials and Methods. A total of 10^5 cpm of ^{125}I-EGF (3×10^4 cpm/pmol) was used per dish. Cold EGF at 3-, 10-, and 50-fold concentrations of the ^{125}I-EGF was premixed and added to the binding assays. The basal level of 110 cpm bound to the equivalent number of control 3T3 cells was subtracted from the values for ER1 and ER2 cells. (C) Scatchard plot of the data shown in panel B. Symbols for panels B and C: circles, ER1 clone 2; triangles, ER1 clone 8; diamonds, ER2 clone 57; X's, ER2 clone 69.

abundances (Fig. 2A). The subcellular distribution of the fusion receptors was examined by fractionation of the cellular extracts and cell surface protein labeling. The results show that independent ER1 and ER2 clones express similar levels of the 160-kDa chimeric receptors which associate mostly with the P100 membrane fraction and could be detected on the cell surface at comparable abundances among the clones (Fig. 2A).

EGF binding and kinetics of chimera activation. The binding of EGF to ER1 and ER2 was analyzed by using ^{125}I-labeled EGF. Independent clones of ER1 and ER2 showed that they had similar binding kinetics for EGF although the absolute capacity of binding varied somewhat among clones (Fig. 2B). From the Scatchard plot, the number of EGF binding sites was estimated to be 0.88×10^5 per cell for both ER1 and ER2 clones. Under similar conditions in parallel experiments, the number of EGF binding sites for A431 cells was determined to be 3.3×10^6 per cell (data not shown). This result agrees with the similar abundance and surface localization of the ER1 and ER2 receptors described above. The Scatchard plot revealed that the binding proceeded in biphase kinetics. However, the affinity appeared to be similar among the clones. The reason for the biphase kinetics is not clear, but it may imply that some chimeric receptors may exist as high-affinity forms, such as dimers, on the cell surface.

Both chimeras could be activated in as rapidly as 30 s by EGF, and the activity increased proportionally to the dosage of EGF as shown by in vitro kinase assay and intracellular tyrosine phosphorylation (Fig. 3). The physical amount of the receptors remained constant during the course of the stimulation. Maximal stimulation of the receptor kinase activity was reached with 50 ng of EGF per ml, which is a severalfold molar excess over the binding sites of ER1 and ER2 cells used in the experiment. After stimulation at the saturation concentration for more than 10 min, in vitro kinase activities of both chimeras started to decrease, presumably because of increased phosphorylation of the major autophosphorylation sites intracellularly, thereby precluding their in vitro phosphorylation.

Both chimeras induce colony formation, but ER1 inhibits whereas ER2 stimulates cell growth on monolayer culture. Two independent clones each from ER1 and ER2 cells were analyzed for their colony-forming abilities. The result showed that both chimeras induced colony formation with about equal efficiency in an EGF-dependent manner, although ER2 had a higher basal level activity (Table 1 and Fig. 4). No significant

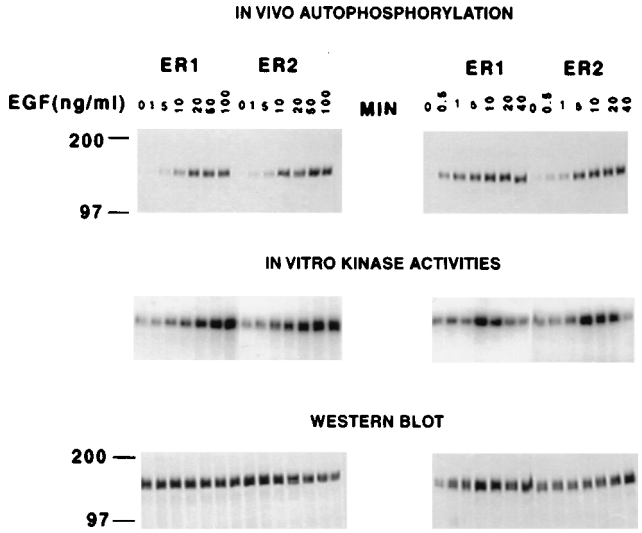

FIG. 3. Kinetics of chimera activation. ER1 and ER2 cells were serum starved overnight and treated either with different amounts of EGF as indicated for 10 min or for different times with 100 ng of EGF per ml. Cells were then lysed, and 0.8 mg of protein from each sample was used for IP with anti-Ros Ab. Half of the immunoprecipitates were used for Western blotting with RC-20 to detect in vivo phosphorylation. The remaining immunoprecipitates were used for in vitro kinase assay and Western blotting with anti-Ros Ab. Numbers at left indicate molecular mass in kilodaltons.

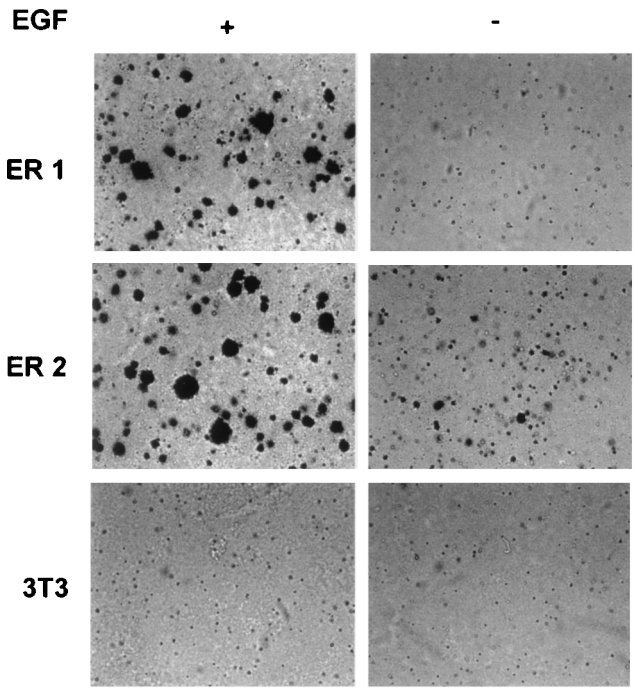

FIG. 4. Colony formation assay. Two individual clones each of ER1 and ER2 cells and control NIH 3T3 cells were seeded in soft agar at 10^5 cells per 60-mm dish in the presence or absence of 10 ng of EGF per ml. Every 5 days, the cells were overlaid with soft agar medium containing either 0.5% serum or 0.5% serum plus 10 ng of EGF per ml. Colonies were counted and pictures were taken after 20 days of incubation. Clones ER1-2, ER2-69, and 3T3-1 are shown.

difference in the size and time of appearance of colonies was observed between ER1 and ER2 clones.

Growth rates of the chimera-expressing cells were determined in the presence or absence of EGF. To our surprise, the two chimeras have opposite effects on cell growth in response to EGF. ER1 inhibits whereas ER2 stimulates cell growth. The opposite effects were not due to clonal variation as all three independent ER1 clones were growth inhibited in response to EGF, whereas all three ER2 clones were stimulated upon EGF treatment (Fig. 5A). The opposite effects on cell growth could be detected when cells were treated with EGF at a concentration as low as 0.25 ng/ml, and the effect was dosage dependent (Fig. 5B). Neither increase of serum concentration (Fig. 5B) nor the addition of IGF-1 (data not shown) could overcome the inhibitory effect. The medium harvested from ER2 culture after 2 days of incubation with EGF could not rescue the EGF-mediated inhibition of ER1 cells. Conversely, similarly conditioned medium from ER1 culture had no effect on ER2 cells (data not shown). The growth inhibition of ER1 is somewhat paradoxical in light of its colony-promoting ability. The ER1 and ER2 cells were tested for anchorage-independent growth in the medium containing 1.3% methylcellulose in the presence or absence of EGF. Under such conditions, EGF stimulated growth of both ER1 and ER2 cells (data not shown). This is consistent with the colony-promoting activity of both chimeras. This result also indicates that ER1-mediated growth inhibition appears to be cell adhesion dependent.

TABLE 1. Colony formation assay[a]

Clone	No. of colonies formed	
	+ EGF	− EGF
ER1-2	1,396	8
ER1-8	1,316	8
ER2-51	1,964	208
ER2-69	1,872	480
3T3-1	82	10
3T3-2	72	8

[a] The experiment is described in the legend to Fig. 3.

Morphology of the chimera-expressing cells changed dramatically in response to EGF treatment. Upon addition of EGF, ER1 and ER2 cells were transformed into more elongated shapes and had a tendency to aggregate into clusters of cells. However, the ER1 cells had proportionally more giant cells (Fig. 6), implying failure of those cells to undergo proper cell division.

Cell detachment of the chimera-expressing lines in the presence or absence of EGF was monitored by counting cells in the medium. No obvious difference was noticed before and after EGF treatment (data not shown), indicating that growth inhibition was not due to increased detachment of ER1 cells in the presence of EGF. DNA fragmentation, a hallmark of apoptosis, was analyzed by gel electrophoresis of genomic DNA extracted from the chimera-expressing cells treated with EGF for 2 days. No DNA fragmentation was observed in either ER1- or ER2-expressing lines (data not shown), indicating that apoptosis was not responsible for the growth inhibition of ER1 cells.

Cell phases are elongated in ER1 cells whereas G_1 phase is shortened in ER2 cells in response to EGF. To explore the mechanism of opposite effects on cell growth by the two chimeras, we analyzed, by flow cytometry, cell cycle distribution of the chimera-expressing cells in response to EGF. The result showed that ER1 cells had a slightly reduced proportion of cells in G_1 phase and a slightly increased proportion of cells in S and G_2/M phases in response to EGF (Table 2). In the case of ER2, the proportion of cells in G_1 phase was decreased by 30% but increased two- to threefold in S and G_2/M phases. The

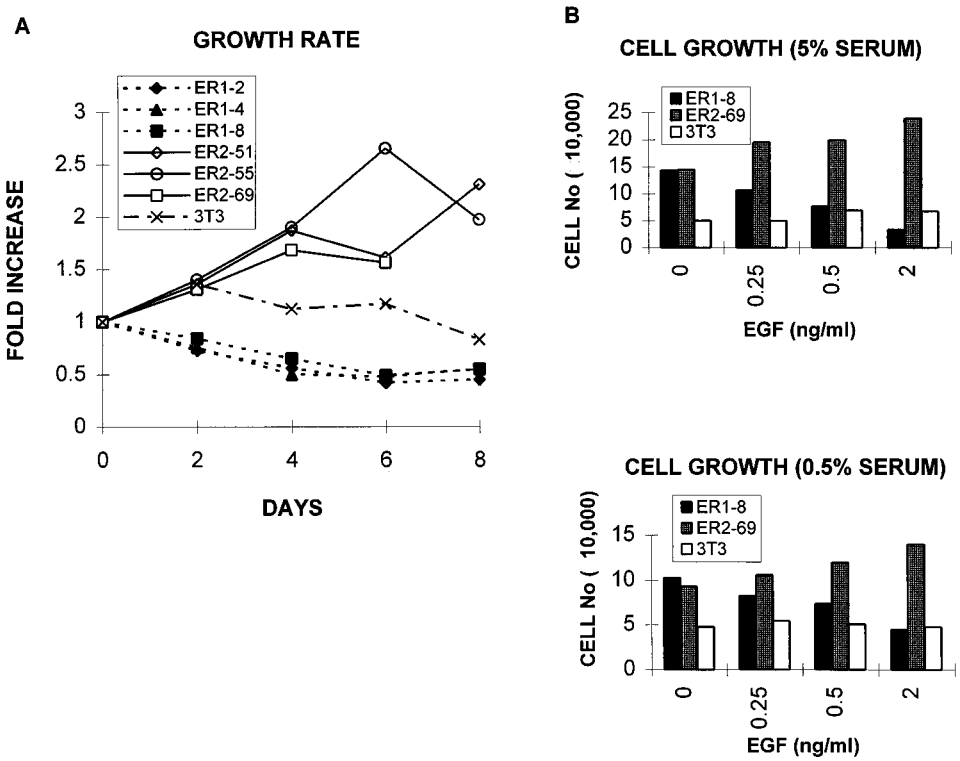

FIG. 5. Growth rate of chimera-expressing cells. (A) Cells were grown in medium containing either 0.5% serum or 0.5% serum plus 10 ng of EGF per ml. Cell numbers were counted every other day. Three individual clones each of ER1 (no. 2, 4, and 8) and ER2 (no. 51, 55, and 69) cells and a control NIH 3T3 clone were analyzed. Day 0 is defined as when EGF treatment started. Mean values of duplicate experiments are expressed as ratios over the control without EGF treatment. (B) Cells were incubated in medium supplemented with either 5% (upper panel) or 0.5% (lower panel) calf serum plus different amounts of EGF as indicated. Cell numbers at day 3 are shown.

doubling times of ER1 cells were determined to be 60 h without EGF and 91 h with EGF treatment. By contrast, EGF treatment of ER2 cells shortened their doubling times from 77 to 38 h. From the cell cycle data in Table 2 and the doubling times, the duration of each phase of the cell cycle was calculated (Table 3). All phases of the cell cycle were elongated after EGF treatment in ER1 cells, especially S and G_2/M phases, which were approximately doubled. By contrast, the duration of G_1 phase was reduced by threefold in ER2 cells after EGF treatment whereas those of S and G_2/M phases remained essentially the same.

ER1 is less efficiently internalized and remains phosphorylated for a longer time than ER2 after EGF treatment. The two chimera-expressing lines were analyzed for internalization of chimera receptors after EGF treatment for various times. The result showed that ER1 was much less efficiently internalized than ER2 (Fig. 7A). After 2 h of treatment with EGF, about 50% of ER1 still remained on the cell surface as detected by labeling of intact cell surface proteins, while most of the ER2 was internalized at this point. Both chimeras, however, were not degraded upon EGF treatment as detected by Western blotting (Fig. 7A, lower panel).

The phosphorylation states of chimeras after EGF stimulation for 10 min followed by its withdrawal for various times were analyzed. The result showed that ER1 remained tyrosine phosphorylated for a longer time than ER2 after EGF withdrawal (Fig. 7B). Half of ER1 remained phosphorylated after EGF withdrawal for 2 h, whereas half of ER2 was dephosphorylated within 30 min, implying that dephosphorylation of chimeras may occur mainly in the cytoplasm after they are internalized.

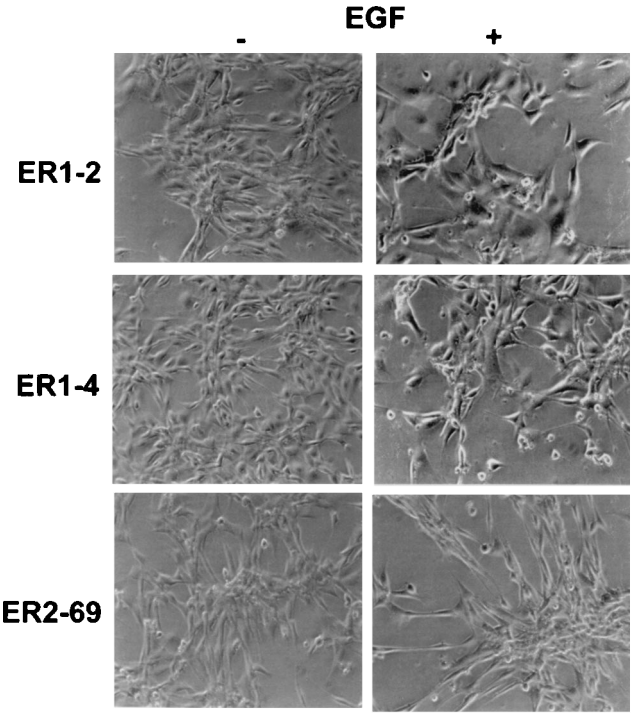

FIG. 6. Morphology of ER1 and ER2 cells in response to EGF treatment. Cells were starved in 0.5% serum overnight and then treated with EGF at 10 ng/ml or left without treatment. Pictures were taken 3 days after treatment with EGF.

TABLE 2. Cell cycle distribution[a]

Cell type	Treatment with EGF	% of cells in phase:		
		G_1	S	G_2/M
ER1	−	66.6 ± 2.5	19.0 ± 1.0	14.2 ± 2.7
	+	56.1 ± 2.3	21.3 ± 2.3	22.3 ± 4.2
ER2	−	81.7 ± 0.1	12.0 ± 0	6.6 ± 0.4
	+	56.9 ± 0.4	26.0 ± 0	17.3 ± 0.1

[a] ER1 and ER2 cells were seeded at 200,000 cells per 6-cm dish. Cells were incubated in medium containing 0.5% serum for 2 days and then treated with EGF at 50 ng/ml for 2 days or left untreated. Cells were counted, and flow cytometry results were analyzed. The means and standard deviations from three independent experiments are shown.

TABLE 3. Duration of each cell phase[a]

Cell type	Treatment with EGF	Cell doubling time (h)	Time (h) in each phase:		
			G_1	S	G_2/M
ER1	−	60 ± 3	40.1 ± 1.5	8.5 ± 0.6	11.4 ± 1.6
	+	91 ± 8	51.0 ± 2.1	20.3 ± 2.1	19.4 ± 3.9
ER2	−	77 ± 4	62.9 ± 0.1	5.1 ± 0	9.2 ± 0.3
	+	38 ± 7	21.6 ± 0.1	6.6 ± 0	9.9 ± 0.1

[a] Calculated from cell cycle distribution (Table 2) and cell doubling times.

Signal transduction by the two chimeras. To understand the molecular mechanism underlying the biological effects of the chimeras, signaling pathways mediated by the chimeras were studied.

IRS1 is an important signaling component of IR family RPTKs (48). Upon phosphorylation, IRS1 functions as an adaptor for SH2 domain-containing proteins, including PI3 kinase and Grb2 (46). Our results showed that IRS1 was phosphorylated in both chimera-expressing cell lines, and to a higher extent in ER1 cells, upon EGF treatment (Fig. 8A).

PLCγ breaks down lipid to generate diacylglycerol and inositol triphosphate, which are involved in protein kinase C activation and calcium mobilization, respectively (3, 51). PLCγ was also phosphorylated in chimera-expressing cells, and also to a higher degree in ER1 cells, in response to EGF treatment (Fig. 8B).

PI3 kinase is involved in mitogenic signaling for many RPTKs (3, 51). The chimera- and IRS1-associated PI3 kinase activity was examined. As shown in Fig. 8C and D, EGF promoted association of PI3 kinase with chimeric receptors and IRS1. Much higher IRS1-associated than chimera receptor-associated PI3 kinase activity was detected. Again, a higher degree of activation, particularly the IRS1-associated PI3 kinase activity, was observed in ER1 cells. A two- to threefold and three- to fourfold increase of IRS1- and Ros-associated PI3 kinase, respectively, was detected upon EGF stimulation.

Activation of MAP kinase, a downstream signaling molecule of the Ras pathway (4), was compared between the two chimera-expressing lines. In both lines, both p42 and p44 species of MAP kinase were phosphorylated in response to EGF as evidenced by mobility upshift in SDS-PAGE (Fig. 9B), and MAP kinase activity increased in response to EGF treatment (Fig. 9A). Quantitative analysis revealed that the MAP kinase activity increased 4.1- and 3.7-fold for ER1 and ER2 cells, respectively, upon EGF stimulation, whereas no significant increase was observed for control 3T3 cells. The duration of MAP kinase activation was also examined (Fig. 9C). In ER1 cells, about 50% of MAP kinase was shifted down after EGF withdrawal for 30 min to 1 h whereas it took 1 to 2 h for ER2 cells to do so. We also examined nuclear translocation of MAPK in response to EGF treatment by immunostaining with an anti-MAP kinase serum. The result showed that MAP kinase was translocated to the nucleus in both chimera-expressing cell lines after EGF treatment for as little as 5 min and remained in the nucleus for at least 1 h (data not shown). Our results showed that IRS1, PLCγ, and PI3 kinase are either phosphorylated or activated to a higher extent in ER1 cells. These results agree with the prolonged activation of ER1 on the cell surface described above. However, the sustained activation of ER1 on the cell surface did not prolong the MAP kinase activation; instead, it appears to have shortened the duration of its activation.

Cellular protein phosphorylation patterns are different between the two chimera-expressing lines upon EGF stimulation. Potential cellular substrates of ER1 and ER2 were analyzed by Western blotting with RC-20. The result showed that the overall tyrosine phosphorylation patterns were similar in both chimera-expressing cell lines in response to EGF treatment (Fig. 10A). However, several proteins were differentially phosphorylated. For example, a protein at about 190 kDa appeared to be preferentially phosphorylated in ER2 cells, whereas the opposite was true for two proteins of less than 43 kDa. At present, we do not know the significance of those differences. Nevertheless, they may suggest that different signaling pathways are triggered by the two chimeras despite their identical cytoplasmic domains.

The 66-kDa Shc and a 190-kDa protein are phosphorylated to a lesser extent in ER1 cells. Shc consists of three species of protein with apparent molecular masses of 46, 52, and 66 kDa (34). We noticed that the 66-kDa species of Shc was phosphorylated to a lesser extent in ER1 cells, whereas the 46- and 52-kDa Shc proteins were equally phosphorylated in both chimera-expressing cell lines in response to EGF (Fig. 10B). Interestingly, a 190-kDa protein could be detected in the anti-Shc immunocomplex after EGF treatment in ER2 but not in ER1 cells. Further experiments suggested that this 190-kDa protein was not the chimera itself or IRS1 (data not shown). Differential phosphorylation of the 66-kDa Shc and 190-kDa protein provides other evidence that the two chimeras have different signaling specificities.

Induction of c-*jun* and c-*fos* by the two chimeras. Induction of c-*jun* and c-*fos* was analyzed in chimera-expressing cells

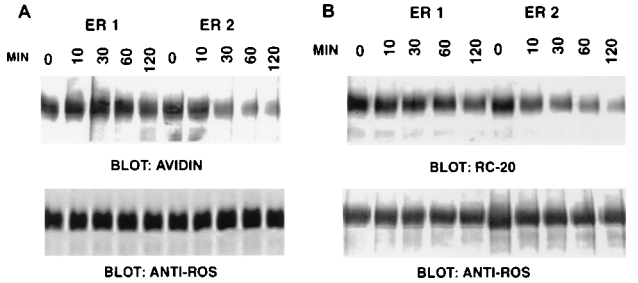

FIG. 7. Internalization and tyrosine phosphorylation of ER1 and ER2 upon EGF treatment. (A) ER1 and ER2 cells were serum starved overnight and treated with EGF for the indicated times. Cells were labeled with biotin, labeling being followed by IP with anti-Ros Ab and Western blotting with avidin conjugated with alkaline phosphatase (upper panel) or anti-Ros Ab (lower panel). (B) ER1 and ER2 cells were stimulated with 100 ng of EGF per ml for 10 min. Then, EGF was washed away and cells were incubated with serum-free medium for the indicated times before they were lysed and immunoprecipitated with anti-Ros Ab and then Western blotted with RC-20 (upper panel) or anti-Ros Ab (lower panel).

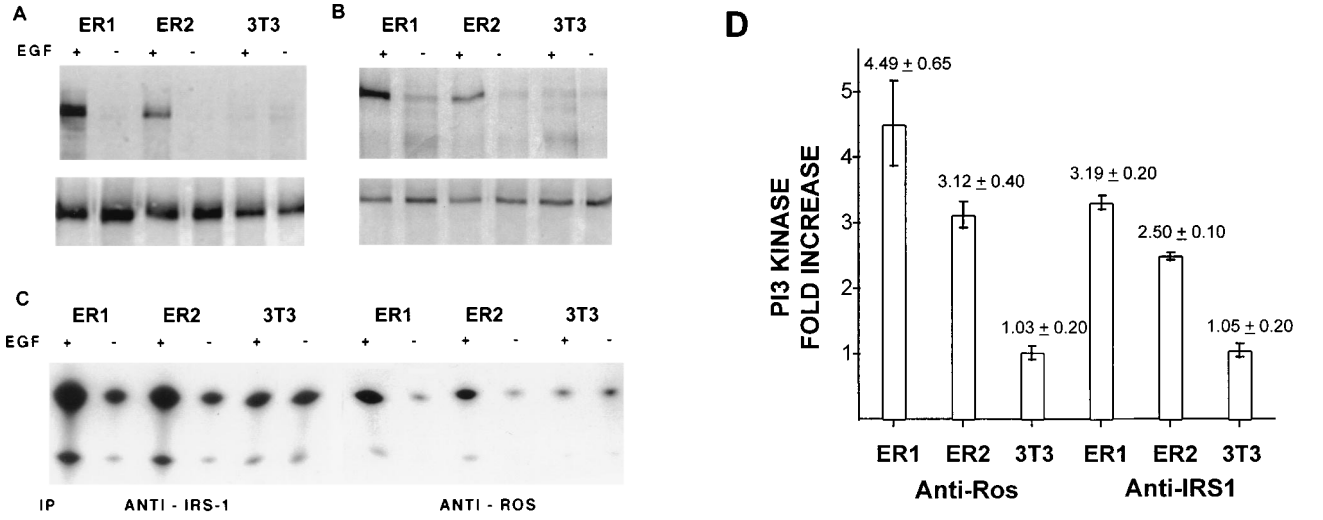

FIG. 8. Tyrosine phosphorylation of IRS1 and PLCγ and activation of PI3 kinase. Cells were serum starved overnight and stimulated with 100 ng of EGF per ml for 10 min or not treated. (A and B) To detect tyrosine phosphorylation, lysates were immunoprecipitated with either anti-IRS1 (A) or anti-PLCγ (B) Ab, followed by SDS–7.5% PAGE and Western blotting with RC-20 (A and B, upper panels), anti-IRS1 (A, lower panel), or anti-PLCγ (B, lower panel). (C) For PI3 kinase assay, cells were lysed with 1% Nonidet P-40 buffer and immunoprecipitated with either anti-IRS1 or anti-Ros Ab. The IRS1- or chimera-associated PI3 kinase activity was measured as described in Materials and Methods. (D) The histogram represents the quantitative analysis of the signals shown in panel C and another experiment not shown here.

after EGF treatment for different times (Fig. 11). Both c-*jun* and c-*fos* were induced in ER1 and ER2 cells. However, the induction of c-*fos* was much less prominent in ER1 cells than that in ER2 cells, and the induction of c-*jun* in ER2 cells lasted longer than that in ER1 cells. The kinetics of c-*jun* induction correlates with the duration of MAP kinase activation shown above. No kinetic difference of c-*fos* induction was observed between the two chimera-expressing lines. However, the interval between two time points in this experiment might be too far apart to reveal the difference since c-*fos* has a very short half-life.

DISCUSSION

Our data showed that the two EGFR-Ros chimeras differing in their TM domains have opposite effects on cell growth on monolayer culture despite their similar transforming abilities. Our results for ER2 are in agreement with a previous study on the NGFR-Ros chimera receptor (42). However, our data demonstrate that the TM domain has a profound effect on the signaling specificity and function of an RPTK, corroborating our previous study of a TM domain mutant of *ros* (54).

A similar growth-inhibitory effect of other RPTKs has been observed. Activation of EGFR promotes cell growth in a number of cell types (15). However, the addition of EGF to A431 and other tumor cell lines overexpressing EGFR resulted in remarkable growth inhibition without any effect on their transformed morphology (12, 13, 19, 20). Hepatocellular carcinoma cells are also growth inhibited upon treatment with hepatocyte growth factor (45).

Multiple possibilities may account for the opposite growth effects of ER1 and ER2. It could be that the genetic differences between ER1 and ER2 clones render ER1 cells susceptible to EGF-mediated inhibition. However, similar behavior of independent clones argues strongly against this possibility. Although some early signaling proteins are activated to a higher extent in ER1 cells, it is still possible that ER1 fails to activate a critical signaling component(s) required for cell growth such as the 66-kDa Shc and the 190-kDa protein. In addition, activation of MAP kinase and induction of early responsive genes are either to a lesser extent or for a shorter time in ER1 cells. However, failure to activate a signaling component(s) may only render cells unresponsive but not growth inhibited. Furthermore, the fact that increase of serum concentration and the addition of IGF-1 fail to rescue the inhibitory effect suggests

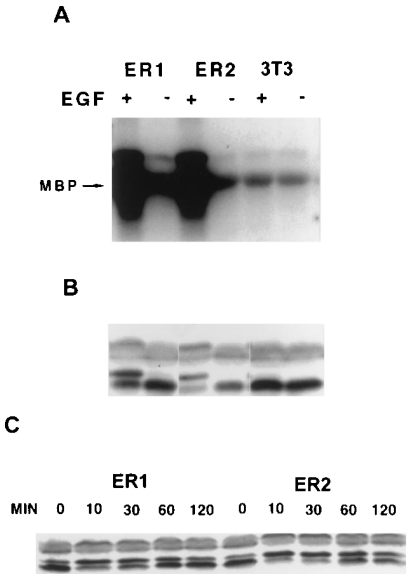

FIG. 9. Activation of MAP kinase. Serum-starved cells were treated with 100 ng of EGF per ml for 10 min before cells were lysed with radioimmunoprecipitation assay buffer containing 0.1% SDS. (A) Activation of MAP kinase by the chimeras. For MAP kinase assay, lysates were immunoprecipitated with TR-10 Ab and MAP kinase activity assay was done as described in Materials and Methods. Labeled myelin basic proteins (MBP) were visualized by SDS–15% PAGE, followed by autoradiography. (B) Mobility shift of MAP kinase. Twenty micrograms of total cell lysates was loaded onto an SDS–10% polyacrylamide gel (bisacrylamide/acrylamide ratio equals 1:77) and Western blotted with anti-ERK-1 Ab. (C) Duration of MAP kinase phosphorylation. Cells were stimulated with 100 ng of EGF per ml for 10 min and then washed with serum-free medium to remove EGF. Cells were then incubated in serum-free medium for different times before lysis for Western blotting. Quantitative analysis of the signals of MAP kinase assay shown here indicated that the increases of activity for ER1, ER2, and 3T3 cells are 4.1-, 3.7-, and 1.1-fold, respectively.

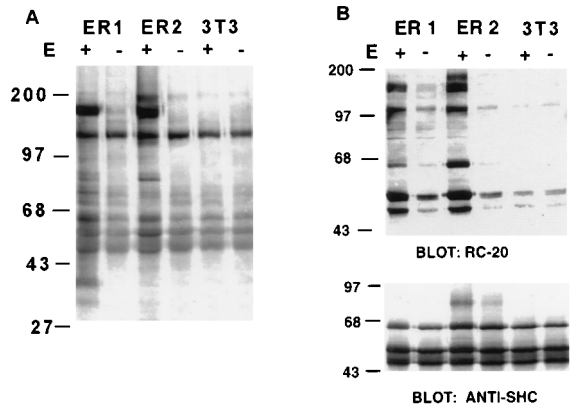

FIG. 10. (A) Cellular protein tyrosine phosphorylation. Cells were serum starved overnight and treated with 100 ng of EGF per ml for 10 min. Cells were lysed, and equal amounts of protein were used for IP with antiphosphotyrosine monoclonal Ab 4G10, followed by SDS-PAGE and blotting with RC-20. (B) Shc phosphorylation. Cell lysates were immunoprecipitated with anti-Shc Ab and then subjected to SDS-PAGE and Western blotting with either RC-20 (upper panel) or anti-Shc (lower panel). Numbers at the left of each panel indicate molecular mass in kilodaltons.

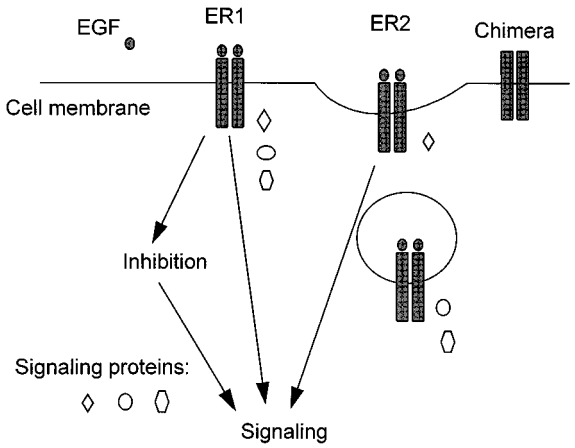

FIG. 12. Schematic diagram of signaling pathways mediated by ER1 and ER2. After EGF binding, ER2, which is internalized efficiently, sends positive signals for cell growth. ER1, which is less efficiently internalized, triggers an inhibitory signal that counteracts the positive signals.

that an inhibitory signal triggered by ER1 dominantly counteracts the positive effect. This inhibitory signal appears to require adhesion of cells to culture dishes since growth inhibition was not observed when cells were grown in methylcellulose medium and both chimeras promote colony formation in agar medium equally well.

Variants derived from EGFR-overexpressing squamous cell carcinoma lines that are resistant to EGF-mediated cell growth inhibition either lose their amplified EGFR gene or are capable of internalizing the cell surface receptors more efficiently (19). Those observations, together with our data, suggest that overstimulation of an RPTK may be responsible for the inhibitory effect. Consistent with this model, the ER1 cells that are growth inhibited by EGF exhibit less efficient receptor internalization, allowing the receptor to remain activated for a longer duration on the cell surface. In addition, several early signaling proteins of RPTKs, including IRS1, PLCγ, and PI3 kinase, are activated to a greater extent in ER1 cells. With the wealth of information about growth-stimulatory function of those signaling components, it is unlikely that overstimulation of an RPTK per se is directly responsible for the growth-inhibitory effect. The identity of a specific signaling molecule(s) mediating the growth arrest or cell-differentiating function of RPTKs remains rather provisional and needs to be explored. Alternatively, receptor stimulation requires rapid down regulation as a physiological response to an activated RPTK. The retarded internalization of ER1 disrupts this normal physiological response and may somehow triggers an inhibitory signal(s) to counteract the overstimulated receptor. When reaching a threshold, the inhibitory component eventually overrides the positive signals elicited by ER1 activation and results in growth inhibition (Fig. 12). The inhibition signal apparently does not act on the proximal signaling events since several immediate substrates are highly activated or phosphorylated in ER1 cells. It is tempting to speculate that the putative inhibitory signal(s) initiates via interaction of a cell surface molecule(s) with those on the substratum because cell adhesion appears to be required for the observed growth-inhibitory phenomenon.

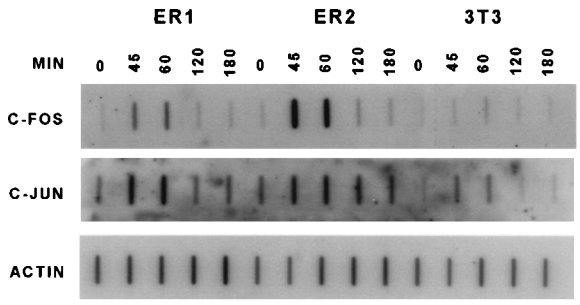

FIG. 11. Induction of c-*fos* and c-*jun* after EGF treatment. ER1, ER2, and 3T3 control cells were serum starved overnight and stimulated with 50 ng of EGF per ml for the indicated times. Then total RNA was extracted and analyzed for c-*fos* and c-*jun* by slot blot hybridization with rat c-*fos*, human c-*jun*, and mouse actin cDNA probes.

The current model of cell cycle control holds that transitions between different cell cycle states are regulated at checkpoints (20, 35, 44). One of the most important checkpoints is START (also known as the restriction point in mammalian cells) in late G_1. Cells are sensitive to a variety of external signals including growth factors until they reach the restriction point late in G_1 after which they can complete division cycle even if only supplied with factors supporting their viability (37). Consistent with this notion, EGF treatment of ER2 cells greatly shortens the G_1 phase, leaving the S and G_2/M phases essentially unchanged. However, EGF-mediated growth inhibition of ER1 cells affects all phases of the cell cycle, particularly the S and G_2/M phases. The appearance of giant cells also suggests that normal mitosis may be blocked. In addition, G_1 phase appears to be affected to some extent also. Interestingly, it was reported that all phases of the cell cycle were elongated in mouse embryo fibroblasts carrying a null mutation of IGFR in comparison with normal mouse embryo fibroblasts (43).

Comparison of signaling pathways mediated by the two chimeras revealed several differences. They are as follows. (i) ER1 is prolonged in tyrosine phosphorylation and delayed in internalization, and several early signaling proteins are activated to a greater extent in cells that express it. (ii) Activation of ER1 and ER2 leads to distinct cellular protein tyrosine phosphorylation patterns. (iii) The phosphorylation of the 66-kDa Shc and a 190-kDa protein is much reduced or lacking in ER1 cells upon EGF stimulation. (iv) Activation of MAP ki-

nase and induction of c-*jun* and c-*fos* are either to a lesser extent or for a shorter time in ER1 cells. However, MAP kinase is rapidly translocated to the nucleus in both ER1 and ER2 cells (data not shown). These observations suggest that the two chimeras have different signaling specificities despite their identical cytoplasmic domains. The difference could be attributed only to the TM and its immediate neighboring sequences (often the TM domain is not precisely defined). The internalization signal of ER1 may be disrupted by fusion of the TM domain of EGFR with the cytoplasmic domain of c-Ros. In support of this notion, the TM and subtransmembrane domains of a number of RPTKs have been reported to be important for their internalization (1, 7, 14, 17, 24, 31, 33, 38, 39). Since ER1 is less efficiently internalized, it remains activated on the cell surface for a longer time and thus has a longer time to interact with its immediate substrates. This could account for the greater extent of phosphorylation or activation of IRS1, PI3 kinase, PLCγ, and some unidentified proteins in ER1 cells. However, this cannot explain why the 66-kDa Shc is less phosphorylated and the duration of MAP kinase is shorter in ER1 cells. It is possible that activation of MAP kinase and Shc and induction of c-*fos* and c-*jun* are counteracted by an inhibitory pathway triggered by ER1 as mentioned above. Alternatively, substitution of the TM domain of c-Ros with that of EGFR may have disrupted the structural integrity of Ros, and as a consequence, the conformation of the cytoplasmic domain of ER1 is different from that of ER2, leading to distinct substrate interactions and signaling specificities. This changed specificity may contribute to the inhibitory effect.

Inhibition of cell growth by activation of an RPTK has been well documented, but little is known about the mechanism. The present study showed that the two chimeras expressing at similar levels in the same cell type have opposite effects on cell growth but similar transforming abilities. Therefore, the two chimera-expressing lines provide an ideal system to further dissect the mechanisms by which an RPTK inhibits or stimulates cell growth. The differential phosphorylation of several cellular proteins including the 66-kDa Shc and a 190-kDa protein may provide a clue towards the understanding of the opposite effects on cell growth induced by the two chimeras.

ACKNOWLEDGMENTS

We thank M. Shibuya for the gift of the pZIPER plasmid; M. Weber for anti-MAP kinase TR-10; I. Gelman and S. Chen-Kiang for cDNAs of c-*jun* and c-*fos*, respectively; T. Moran for assistance in the preparation of ^{125}I-EGF; and R. Krauss for information on the conditions for growing cells in methylcellulose medium.

This work was supported by a grant from the NIH (CA29339).

REFERENCES

1. **Berharu, P., A. M. Rohilla, and W. J. Rutter.** 1990. Replacement of the human insulin receptor transmembrane and cytoplasmic domains by corresponding domains of the oncogene product v-ros leads to accelerated internalization, degradation and down regulation. J. Biol. Chem. **265:**9505–9511.
2. **Birchmeier, C., K. O'Neill, M. Riggs, and M. Wigler.** 1990. Characterization of *ROS* 1 cDNA from a human glioblastoma cell line. Proc. Natl. Acad. Sci. USA **87:**4799–4803.
3. **Birchmeier, C., S. Sharma, and M. Wigler.** 1987. Expression and rearrangement of the *ROS1* gene in human glioblastoma cells. Proc. Natl. Acad. Sci. USA **84:**9270–9274.
4. **Cantley, L. C., K. R. Auger, C. Carpenter, B. Duckworth, A. Grazianti, R. Kapeller, and S. Soltoff.** 1991. Oncogenes and signal transduction. Cell **64:**281–302.
5. **Chen, J., M. Heller, B. Poon, L. Kang, and L.-H. Wang.** 1991. The proto-oncogene c-*ros* codes for a transmembrane tyrosine kinase sharing sequence and structural homology with *sevenless* protein of Drosophila melanogaster. Oncogene **6:**257–264.

5a. **Chen, J., and L.-H. Wang.** Unpublished data.

5b. **Chen, J., Q. Xiong, and L.-H. Wang.** Unpublished data.

6. **Chen, J., C. S. Zong, and L.-H. Wang.** 1994. Tissue and epithelial cell-specific expression of chicken proto-oncogene c-*ros* in several organs suggests that it may play roles in their development and mature functions. Oncogene **9:**773–780.
7. **Chen, W. S., L. S. Lazar, K. A. Lund, J. B. Welsh, C. P. Chang, G. M. Walton, L. J. Der, H. S. Wiley, G. N. Gill, and M. G. Rosenfeld.** 1989. Functional independence of the epidermal growth factor receptor from a domain required for ligand-induced internalization and calcium regulation. Cell **59:**33–43.
8. **Di Fiore, P. P., O. Segatto, F. Conardo, F. Fazioli, J. H. Pierce, and S. A. Aaronson.** 1990. The carboxy-terminal domains of *erbB-2* and epidermal growth factor receptor exert different regulatory effects on intrinsic receptor tyrosine kinase function and transforming activity. Mol. Cell. Biol. **10:**2749–2756.
9. **Dikic, I., J. Schlessinger, and I. Lax.** 1994. PC12 cells overexpressing the insulin receptor undergo insulin-dependent neuronal differentiation. Curr. Biol. **4:**702–708.
10. **Ellis, L., E. Clauser, D. O. Morgan, M. Edery, R. A. Roth, and W. J. Rutter.** 1986. Replacement of insulin receptor tyrosine residues 1162 and 1163 compromises insulin-stimulated activity and uptake of 2-deoxyglucose. Cell **45:**721–732.
11. **Feldman, R. A., L.-H. Wang, H. Hanafusa, and P. C. Balduzzi.** 1982. Avian sarcoma virus UR2 encodes a transforming protein which is associated with a unique protein kinase activity. J. Virol. **42:**128–136.
12. **Filmus, J., J. M. Trent, M. N. Pollak, and R. N. Buick.** 1987. Epidermal growth factor receptor gene-amplified MDA-468 breast cancer cell line and its nonamplified variants. Mol. Cell. Biol. **7:**251–257.
13. **Gill, G. N., and L. S. Lazar.** 1981. Increased phosphotyrosine content and inhibition of proliferation in EGF-treated A431 cells. Nature (London) **293:**305–307.
14. **Gonclalves, E., K. Yamada, H. S. Thatte, J. M. Backer, D. E. Golan, C. R. Kahn, and S. E. Shoelson.** 1993. Optimizing transmembrane domain helicity accelerates insulin receptor internalization and lateral mobility. Proc. Natl. Acad. Sci. USA **90:**5762–5766.
15. **Gospodarowicz, D., G. Greenburg, H. Biaslecki, and B. R. Zether.** 1978. Factors involved in the modulation of cell proliferation in vivo and in vitro: the role of fibroblast and epidermal growth factors in the proliferative response of mammalian cells. In Vitro (Rockville) **14:**85–118.
16. **Graham, F. L., and A. J. Van Der Eb.** 1973. A new technique for the assay of infectivity of human adenovirus DNA. Virology **52:**456–467.
17. **Haft, C. R., R. D. Klausner, and S. I. Taylor.** 1994. Involvement of dileucine motifs in the internalization and degradation of the insulin receptor. J. Biol. Chem. **269:**26286–26294.
18. **Hanafusa, H.** 1969. Rapid transformation of cells by Rous sarcoma virus. Proc. Natl. Acad. Sci. USA **63:**318–325.
19. **Hirai, M., S. Gamous, S. Minoshima, and N. Shimizu.** 1988. Two independent mechanisms for escaping EGF-mediated growth inhibition in EGFR-hyperproducing human tumor cells. J. Cell Biol. **107:**791–799.
20. **Hunter, T., and J. Pines.** 1995. Cyclins and cancer II: cyclin D and CDK inhibitors. Cell **79:**573–582.

20a. **Jiang, Y., J. Chan, C. Zong, and L.-H. Wang.** Unpublished data.

21. **Jong, S. M., and L.-H. Wang.** 1987. The transforming protein p68$^{gag\text{-}ros}$ of avian sarcoma virus UR2 is a transmembrane protein with the gag protein protruding extracellularly. Oncogene Res. **1:**7–21.
22. **Jong, S. M., and L.-H. Wang.** 1990. Role of *gag* sequence in the biochemical properties and transforming activity of the avian sarcoma virus UR2-encoded *gag-ros* fusion protein. J. Virol. **64:**5997–6009.
23. **Jong, S. M., and L.-H. Wang.** 1991. Two point mutations in the transmembrane domain of P68$^{gag\text{-}ros}$ inactivate its transforming activity and cause a delay in membrane association. J. Virol. **65:**180–189.
24. **Kaburagi, Y., K. Momomura, R. Yamamoto-Honda, K. Tobe, Y. Tamor, H. Sakura, Y. Akanuma, Y. Yazaki, and T. Kadowaki.** 1993. Site-directed mutagenesis of the juxtamembrane domain of the human insulin receptor. J. Biol. Chem. **268:**16610–16622.
25. **Kraus, M. H., P. Fedi, V. Starks, R. Muraro, and S. A. Aaronson.** 1993. Demonstration of ligand-dependent signaling by the erbB3 tyrosine kinase and its constitutive activation in human breast tumor cells. Proc. Natl. Acad. Sci. USA **90:**2900–2904.
26. **Lammers, R., A. Gray, J. Schlessinger, and A. Ullrich.** 1989. Differential signaling potential of insulin and IGF1-receptor cytoplasmic domains. EMBO J. **8:**1369–1375.
27. **Lehvaslaiho, H., L. Lehtola, L. Sistonen, and K. Alitalo.** 1989. A chimeric EGFR-neu proto-oncogene allows EGF to regulate Neu tyrosine kinase and cell transformation. EMBO J. **8:**159–166.
28. **Lhotak, V., and T. Pawson.** 1993. Biological and biochemical activities of a chimeric epidermal growth factor-Elk receptor tyrosine kinase. Mol. Cell. Biol. **13:**7071–7079.
29. **Lifshitz, A., L. S. Lazar, J. Buss, and G. N. Gill.** 1983. Analysis of morphology and receptor metabolism in clonal variant A431 cells with differing growth response to EGF. J. Cell. Physiol. **115:**235–242.
30. **Liu, D.-L., W. J. Rutter, and L.-H. Wang.** 1993. Modulating effects of the extracellular sequence of the human insulin-like growth factor 1 receptor on

its transforming and tumorigenic potential. J. Virol. **67:**9–18.
31. **Lund, K. A., L. S. Lazar, W. S. Chen, B. J. Walsh, J. B. Welsh, J. J. Herbst, G. M. Walton, M. G. Rosenfeld, G. N. Gill, and H. S. Wiley.** 1990. Phosphorylation of the epidermal growth factor receptor at threonine 654 inhibits ligand-mediated internalization and down-regulation. J. Biol. Chem. **265:** 20517–20523.
32. **Matsushime, H., and M. Shibuya.** 1990. Tissue-specific expression of rat c-*ros-1* gene and partial structural similarity of its predicted products with *sev* protein of *Drosophila melanogaster*. J. Virol. **64:**2117–2125.
33. **Mori, S., L. Claesson-Welsh, and L. H. Heldin.** 1991. Identification of a hydrophobic region in the carboxyl terminus of the platelet-derived growth factor beta-receptor which is important for ligand-mediated endocytosis. J. Biol. Chem. **266:**21156–21164.
34. **Nicoletti, I., F. Gribnani, T. Pawson, and P. G. Pelicci.** 1992. A novel transforming protein (Shc) with an SH2 domain is implicated in mitogen transduction. Cell **70:**93–104.
35. **Nurse, P.** 1995. Ordering S phase and M phase in the cell cycle. Cell **79:** 547–550.
36. **Pandiella, A., H. Lehvaslaiho, M. Magni, K. Altitalo, and J. Meldolesi.** 1989. Activation of an EGFR/Neu chimeric receptor: early intracellular signals and cell proliferation responses. Oncogene **4:**1299–1305.
37. **Pardee, A. B.** 1989. G1 events and regulation of cell proliferation. Science **246:**603–608.
38. **Prager, D., H.-L. Li, H. Yamasaki, and S. Melmed.** 1994. Human insulin-like growth factor 1 receptor internalization: role of the juxtamembrane domain. J. Biol. Chem. **269:**11934–11937.
39. **Rajagopalan, M., J. L. Neidigh, and D. A. McClain.** 1991. Amino acid sequence Gly-Pro-Leu-Tyr and Asn-Pro-Glu-Tyr in the submembrane domain of the insulin receptor are required for normal endocytosis. J. Biol. Chem. **266:**23068–23073.
40. **Riedel, H., T. J. Dull, A. M. Honegger, J. Schlessinger, and A. Ullrich.** 1989. Cytoplasmic domains determine signal specificity, cellular routing characteristics and influence ligand binding of epidermal growth factor and insulin receptors. EMBO J. **8:**2943–2954.
41. **Riedel, H., T. J. Dull, J. Schlessinger, and A. Ullrich.** 1986. A chimeric receptor allows insulin to stimulate tyrosine kinase activity of epidermal growth factor receptor. Nature (London) **324:**68–70.
42. **Riethmacher, D., O. Langhalz, S. Goddecke, M. Sachs, and L. Birchmeier.** 1994. Biochemical and functional characterization of the murine *ros* protooncogene. Oncogene **9:**3617–3626.
43. **Sell, L., G. Dumenil, L. Deveaud, M. Miura, D. Coppola, T. DeAngelis, R. Rubin, A. Efstratiadis, and R. Baserga.** 1994. Effect of a null mutation of the insulin-like growth factor I receptor gene on growth and transformation of mouse embryo fibroblasts. Mol. Cell. Biol. **14:**3604–3612.
44. **Sherr, C. J.** 1995. G1 phase progression: cycling on cue. Cell **79:**551–555.
45. **Shiota, G., D. B. Rhoad, T. C. Wang, T. Nakamura, and E. V. Schmidt.** 1992. Hepatocyte growth factor inhibits growth of hepatocellular carcinoma cells. Proc. Natl. Acad. Sci. USA **89:**373–377.
46. **Skolink, E. Y., C. H. Lee, A. Ratzer, et al.** 1993. The SH2/SH3 domain-containing protein Grb2 interacts with tyrosine phosphorylated IRS1 and Shc: implication for insulin control of ras signalling. EMBO J. **12:**1929–1936.
47. **Sonnenberg, E., A. Godecke, B. Walter, F. Bladt, and C. Birchmeier.** 1991. Transient and locally restricted expression of the *ros*1 proto-oncogene during mouse development. EMBO J. **10:**3693–3702.
48. **Sun, X. J., P. Rothenberg, C. R. Kahn, J. M. Backer, E. Araki, P. A. Wilden, D. A. Cahill, B. J. Goldstein, and M. F. White.** 1991. Structure of the insulin receptor substrate IRS1 defines a unique signal transduction protein. Nature (London) **351:**73–77.
49. **Tessarollo, L., L. Nagarajan, and L. F. Parada.** 1992. c-*ros*: the vertebrate homolog of the *sevenless* tyrosine kinase receptor is tightly regulated during organogenesis in mouse embryonic development. Development **115:**11–20.
50. **Traverse, S., K. Seedorf, H. Paterson, C. J. Marshall, P. Cohen, and A. Ullrich.** 1994. EGF triggers neuronal differentiation of PC12 cells that overexpress the EGF receptor. Curr. Biol. **418:**694–701.
51. **Ullrich, A., and J. Schlessinger.** 1990. Signal transduction by receptors with tyrosine kinase activity. Cell **61:**202–212.
52. **Yan, H., J. Schlessinger, and M. V. Chao.** 1991. Chimeric NGF-EGF receptor define domains responsible for neuronal differentiation. Science **252:** 561–563.
53. **Zong, C. S., B. Poon, J. Chen, and L.-H. Wang.** 1993. Molecular and biochemical bases for activation of the transforming potential of the protooncogene c-*ros*. J. Virol. **67:**6453–6462.
54. **Zong, C. S., and L.-H. Wang.** 1994. Modulatory effect of the transmembrane domain of the protein-tyrosine kinase encoded by oncogene *ros*: biological function and substrate interaction. Proc. Natl. Acad. Sci. USA **91:**10982–10986.